Calibration of lateral force measurements in atomic force microscopy with a piezoresistive force sensor

Hui Xie,[1,a)] Julien Vitard,[1] Sinan Haliyo,[1] Stéphane Régnier,[1] and Mehdi Boukallel[2]
[1]*Institut des Systèmes Intelligents et Robotique (ISIR), Université Pierre et Marie Curie-Paris 6/CNRS, 18 Route du Panorama-BP 61, 92265 Fontenay-Aux-Roses, France*
[2]*Laboratoire de Robotique et Mésorobotique (LRM), CEA, 18 Route du Panorama-BP 61, 92265 Fontenay-Aux-Roses, France*

(Received 28 October 2007; accepted 16 February 2008; published online 19 March 2008)

We present here a method to calibrate the lateral force in the atomic force microscope. This method makes use of an accurately calibrated force sensor composed of a tipless piezoresistive cantilever and corresponding signal amplifying and processing electronics. Two ways of force loading with different loading points were compared by scanning the top and side edges of the piezoresistive cantilever. Conversion factors between the lateral force and photodiode signal using three types of atomic force microscope cantilevers with rectangular geometries (normal spring constants from 0.092 to 1.24 N/m and lateral stiffness from 10.34 to 101.06 N/m) were measured in experiments using the proposed method. When used properly, this method calibrates the conversion factors that are accurate to $\pm 12.4\%$ or better. This standard has less error than the commonly used method based on the cantilever's beam mechanics. Methods such of this allow accurate and direct conversion between lateral forces and photodiode signals without any knowledge of the cantilevers and the laser measuring system. © *2008 American Institute of Physics.* [DOI: 10.1063/1.2894209]

INTRODUCTION

Techniques for the reliable and precise calibration of atomic force microscopes (AFM) have been significant issues since AFM was developed more than two decades ago.[1] There are two categories of AFM calibration: normal force calibration and lateral force calibration. The quantitative determination of absolute values of normal and lateral force conversion factors generally involves two steps: the calibration of photodiode responses and the measurement of cantilever spring constants. The spring constants can be calculated from the geometric and physical properties of the cantilevers[2–4] or modeled by finite-element analysis.[5–7] However, these methods are approximate as ideal models of cantilevers are used (e.g., ideal geometry, coatings not factored in, etc.). Moreover, minor errors in dimension measurements can induce substantial stiffness errors, especially the thickness measurement. Thus, there has been a tendency to determine the cantilever spring constants experimentally.

To measure the normal spring constant, the most commonly adopted method was developed by Cleveland *et al.* who measured frequency shifts due to the known mass loaded on the free end of the cantilevers,[8] although it is thought to be time consuming. Ruan and Bhushan used a stainless steel spring sheet with known stiffness to measure the spring constants of the cantilevers.[9] Recently, Sader *et al.* developed a method to calculate the cantilever's normal spring constant from resonant frequencies induced by thermal fluctuations.[10] More recently still, several methods have been reported for the calibration of the normal constant.[11–15] A newly reported "piezosensor" uses a piezoresistive cantilever as an active force sensor to calibrate the normal spring constants of the AFM cantilevers.[16] A normal force applied to the cantilever's tip can be easily calculated by multiplying the cantilever's vertical deflection to its normal spring constant. Thus, the normal conversion factor can be easily determined by experimental results.

The conversion of lateral force and photodiode signal is more challenging than the normal calibration. Normally, two kinds of methods are used to calibrate the lateral conversion factor: a two-step method and a direct method. The former involves the calibration of the lateral stiffness of the cantilever and the measurement of the lateral photodiode response. This method is not straightforward and is limited in application. Unlike the calibration of the normal constant, the lateral sensitivity of the photodiode is more difficult to determine because the lateral contact stiffness between the AFM tip and the sample surface is proportional to contact radius[17] and often comparable to the lateral stiffness of the cantilever and the tip,[18] which significantly reduces the calibration result of the lateral sensitivity of the photodiode.[19,20] In order to overcome this limitation, several methods have been put forward for lateral sensitivity measurement.[19,21,22] A *test probe* with an attached colloidal sphere was successfully used to determine lateral photodiode sensitivity by loading the colloidal sphere laterally against a vertical sidewall.[20] However, this kind of method is also limited in application because of difficulties in characterization of the lateral stiffness of the V-shaped cantilevers.[23]

In contrast with the two-step method, a one-step direct method, named *wedge* method, developed by Ogletree *et al.* is the most commonly accepted method in current use.[24] This

[a)]Author to whom correspondence should be addressed. Tel.: (33) 01 46 54 92 39. FAX: (33) 01 46 54 72 99. Electronic mail: xie@robot.jussieu.fr.

method gets round the difficulties in the separate measurement of the lateral stiffness of the cantilever and lateral sensitivity of the photodiode. An improved wedge method developed by Varenberg *et al.* utilizes a commercially available calibration grating with a well-defined slope instead of the friction loops generated from different slopes,[25] which enables calibration of all types of probes, including probes integrated with sharp or colloidal tips. A newly reported method based on direct force balances on surfaces with known slopes considers detector cross-talking and off-centered tip problems and reduces tip wear during the calibration.[26] Direct force loading methods, including small glass fibers,[27–29] a specially fabricated microelectromechanical device[30] and magnetic forces[31,32] have been also used to directly calibrate AFM lateral force measurement. Compared with the wedge method, the accuracy of calibration results with these methods is greatly affected by friction forces,[27–29] and the system setup is more technically complex for the experiments.[30,32]

Here, we present a new method to calibrate the lateral force measurement of the AFM using a commercially available, accurately calibrated piezoresistive force sensor. It consists of a piezoresistive cantilever and accompanying electronics, providing a standard force applied on the AFM tip for lateral force calibration. Before use, the spring constant of the piezoresistive cantilever and sensitivity of the accompanying electronics were accurately calibrated. This method may be used to directly calibrate the factor between the lateral force and the photodiode signal for cantilevers with a wide range of spring constants, regardless of their size, shape, material, or coating effects. Three rectangular cantilevers with normal spring constants from 0.092 to 1.24 N/m (lateral stiffness from 10.34 to 101.06) were calibrated. Moreover, we compared the calibration results with the theoretically calculated results based on the beam mechanics, which would yield the best results when the cantilever has a simple geometry and uniform physical properties, and the photodiode has an ideal symmetry of the normal and lateral output.

MATERIAL AND METHODS

Calibration of the piezoresistive force sensor. A piezoresistive cantilever fabricated by the standard silicon bulk micromachining technology with low scatter and drift of sensitivity can be used as a portable microforce calibration standard.[33] The piezoresistive cantilever (Nascatec GmbH, Germany) and its accompanying electronics used in our work are commercially available. Microscopy images of the cantilever are shown in Fig. 1. Dimensions of the piezoresistive cantilever were measured as 525.8 μm in length and with an average width of 152.7 μm using microscopic image processing (under an optical microscope Olympus BX50WI with a 50× objective and Sony XC-711P CCD, providing a resolution of 0.22 μm/pixel). The top view Fig. 1(b) shows that the clamping end of the piezoresistive cantilever has a step shape with a difference of 12.5 μm on the width and a hole with a length of 15 μm on square (maybe for stress enhancement), so it is not convenient to directly calculate its

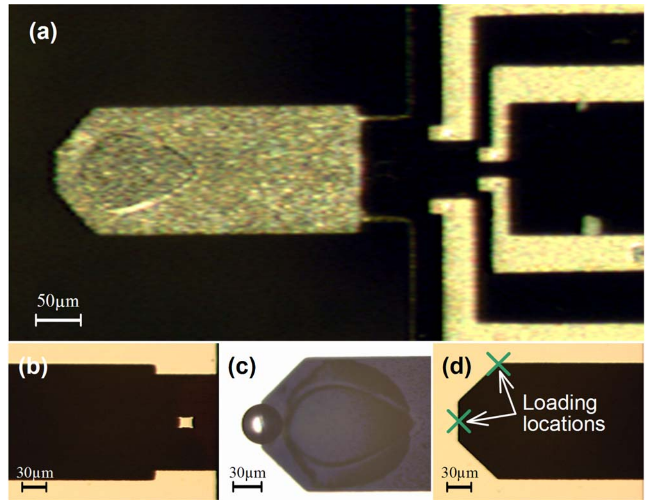

FIG. 1. (Color online) Optical microscopy images of the piezoresistive cantilever used in the calibration of the lateral force measurements. (a) Top image of the piezoresistive cantilever. (b) The shape of the clamping end of the piezoresistive cantilever with a step shape and a hole in its center. (c) An image obtained after a glass microsphere was placed on the tip of the piezoresistive cantilever. (d) A magnified image of the tip in which two loading locations for the lateral calibration are marked. These two locations are close to the end of the side edge and the center point of the top edge on the back of piezoresistive cantilever, respectively.

normal spring constant. Therefore, in our experiment, the piezoresistive cantilever stiffness k_p was calibrated using Cleveland's mass loading method.[8] We used six glass microspheres with diameters from 25.6 to 64.4 μm measured under the optical microscope, and used a glass density of 2.4 g/cm^3. As shown in Fig. 1(c), the glass microspheres were released on the free end of the piezoresistive cantilever and their centers were measured for stiffness compensation due to position errors.[15,16]

Experiments showed that the adhesion force between the glass microspheres and the back side of the piezoresistive cantilever was strong enough to hold the microbeads during the first mode of vibration with very low amplitude (under a humidity of 50%–60%). The first natural resonant frequency of the piezoresistive cantilever is 37.463 kHz. The stiffness of the piezoresistive cantilever was calibrated at $k_p = 18.209 \pm 0.471$ N/m.

The next step is the force calibration of the piezoresistive sensor. The piezoresistive cantilever was mounted horizontally on a three degrees of freedom (DOF) platform, so the force applied on the cantilever was normal to its longitudinal axis. A glass substrate was attached on a *Z* nanopositioning stage with a resolution of 1.8 nm, which was used for the displacement increments during the calibration. On the surface of the glass substrate, a glass microsphere with a diameter of 50 μm was glued near the substrate edge used for the point of contact with the piezoresistive cantilever during the force loading. First, the nanopositioning stage was adjusted by 100 nm increments until the contact between the piezoresistive cantilever tip and the glass microsphere was achieved. The contact point on the horizontal plane was controlled by microscopy vision, while the Wheatstone bridge voltage output was used to detect the contact on the approaching direction. After the contact had been setup, a pro-

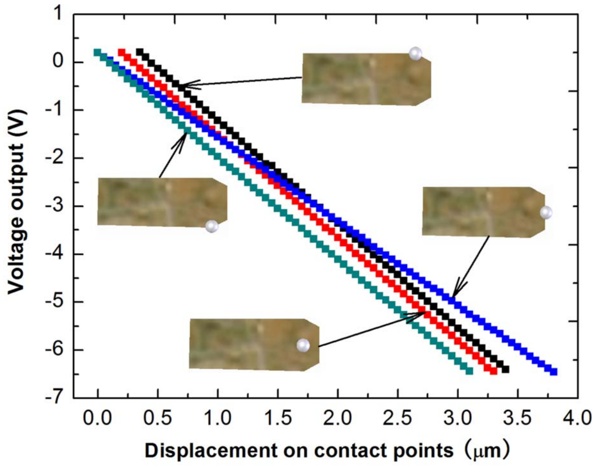

FIG. 2. (Color online) Examples of the sensitivity calibration on four different contact points (see four corresponding scaled images) on the cantilever. In which three curves with the same gradient present the contact points on the hemline of the trapezoid head on the free end of the cantilever. The fourth curve with a lower gradient denotes the calibration result when the contact point is on the tip of cantilever.

gram was used to control the motion of the nanopositioning stage with a fixed increment (20 nm in our experiment) while the voltage output V_p of the electronics was recorded. It was found that the displacement of the piezoresistive cantilever tip was approximately 5.7 μm across the full range of the piezoresistive force sensor output.

After 20 complete loading/unloading calibration cycles, we achieved a piezoresistive force sensor sensitivity $S_p = 10.361 \pm 0.267$ μN/V. The sensitivity $S_p = dF/dV_p$ is defined as the gradient of the applied force F versus the voltage output V_p plot.

During the force calibration of the piezoresistive force sensor, four contact points were used to test whether a position change on the width affects its sensitivity. As shown in Fig. 2, the first three contact points were located on the hemline of the trapezoidal head on the free end, on which there were two points: one on each of the left and right bottom corners, and another in the center of the line. The fourth contact point was located on the very tip of the free end. Plots of the voltage output versus displacement (applied force) have the same gradient except for the fourth contact point, which has a lower gradient because of a lower stiffness on the tip. This experimental result demonstrated that the Wheatstone resistance bridge is not sensitive to the torsion loading applied on the piezoresistive cantilever's longitudinal axis. Thus, the points on the side edges as well as the points on the tip edge of the piezoresistive cantilever can be used as loading locations for the AFM cantilever calibration. This will be discussed below.

Testing AFM cantilevers. Three types of AFM cantilevers with rectangular cross sections and normal force constants from 0.092 to 1.24 N/m (shown in Table I) were used: LFMR (NANO World), ContAL, and Multi75AL (Budget Sensors). Although dimensions of the cantilevers were provided by manufactures, the optical microscope (with 50× and 100× lenses) was used to determine the cantilever's length, width, and tip height. However, the optical microscope's resolution limitation will result in a significant error in the measurement of the cantilever's dimension, especially its thickness. Therefore, in our experiment, the forced oscillation method was employed to determine the cantilever's thickness based on its natural frequency. For the Euler–Bernoulli beam, if we know the resonant frequencies of the cantilevers, the thickness t can be obtained from[34]

$$t = \frac{\omega_n}{K_n^2}\sqrt{\frac{12\rho}{E}}, \tag{1}$$

where K_n is the wave number on the AFM cantilever and ρ is its density and ω_n is the nth flexural resonant frequency. If $n=1$, then $K_nL=1.8751$, where L is the length of the AFM cantilever. When the dimensions of the cantilever are obtained, the normal and lateral spring constants k_n and k_l can be calculated from

$$k_n = \frac{Ewt^3}{4L^3},$$

$$k_l = \frac{Gwt^3}{3L(h+t/2)^2}, \tag{2}$$

where w, t, and h are the width, thickness, and tip height of the AFM cantilever, respectively.

Experimental methods. Once the piezoresistive force sensor had been calibrated, it was used as a force standard to determine the lateral force conversion factor α of the AFM cantilevers. The experiments described below were performed on a combined AFM/optical microscope system. Although the experiment procedure in this work may be not available on all commercial AFMs, this method could be widely used after some adjustment.

For its actual use, the piezoresistive cantilever was fixed into a metal harness with four contact clips. The cantilever and the harness were integrated onto a thin circuit board, which was attached to the AFM stage using a fixture. The electronics, including amplifier, signal filter, and power sup-

TABLE I. Descriptions of the cantilevers based on the beam mechanics and the experimental results. The cantilever's length L, the width w, and the tip height h were measured using the optical microscope. The first flexure resonant frequencies f_0 were used to determine the thickness of the AFM cantilevers from Eq. (1). The normal spring constant k_n and lateral spring constant k_l were calculated from Eq. (2). α_0 calculated based on the beam mechanics from Eq. (11), α measured from the proposed *top loading* and *side loading* methods are listed in the last three columns respectively.

Tip No.	L(μm)	h(μm)	w(μm)	t(μm)	f_0(kHz)	k_n(N/m)	k_l(N/m)	α_0(μN/V)	α(μN/V)	α(μN/V)
1	228	15.5	47.8	0.83	21.84	0.092	10.34	1.61 ± 0.53	2.29 ± 0.26	2.32 ± 0.26
2	449	17.4	53.4	2.01	13.64	0.19	62.27	11.24 ± 3.71	12.04 ± 1.35	12.31 ± 1.38
3	229	17.6	31.4	2.28	59.49	1.24	101.06	18.79 ± 6.20	25.84 ± 2.89	26.2 ± 2.93

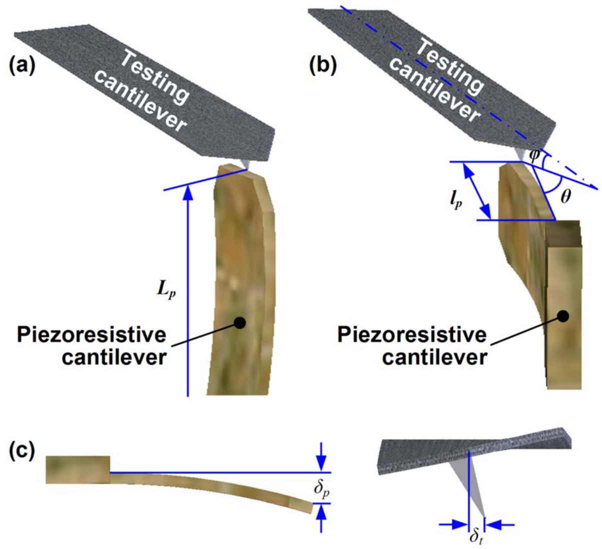

FIG. 3. (Color online) Diagrams of the experimental configurations for the calibration of the AFM cantilevers with a piezoresistive force sensor. Two methods, termed *top loading* (a) and *side loading* (b), in which L_p and l_p are distances from the contact points to the clamping end of the piezoresistive cantilever, φ is the mounting angle of AFM cantilever on the vertical plane that is through its longitudinal axis, and θ is the mounting angle of the piezoresistive cantilever on the horizontal plane. (c) The deflections of the piezoresistive cantilever and AFM cantilever tip are δ_p and δ_t, respectively.

ply, was separated in another unit. Considering the limitations of the manipulation space in the AFM, two ways were recommended for mounting the piezoresistive cantilever. The first involves mounting the piezoresistive cantilever vertically on the AFM stage along its longitudinal axis [see Fig. 3(a)], termed *top loading*, which reduces the mounting area at the cost of height space. In this way, the AFM cantilever tip contacts with the top edge of the piezoresistive cantilever during the calibration [see the loading location in Fig. 1(d)]. Nevertheless, if the piezoresistive cantilever is too high (8 mm in our experiments), the piezoresistive cantilever can be mounted in the second way: horizontally on the AFM stage [see Fig. 3(b)], termed *side loading*. Note that in this case, shoulders of the piezoresistive cantilever substrate might be in the way of the reflected laser beam, so an angle θ to the vertical plane that is through the longitudinal axis of the AFM cantilever was deliberately mounted (θ=15° in our experiments). The loading location in the second method was very close to end of the side edge [see Fig. 1(d)].

Lateral force calibration was started once the whole setup was ready. At first, we had to find the loading locations. For the top loading, after the AFM cantilever was brought into contact with the top surface of the piezoresistive cantilever, the contact mode was used to scan the top side edge to identify its center point. Then the AFM cantilever was moved 2 μm away from the scanned side edge. In order to ensure that the AFM tip was reliably in contact with the top side edge, the AFM cantilever was moved down with a displacement Δh=0.5–0.8 μm before being moved back to the contact location. For the side loading, the procedure was largely the same; the only difference being the position of the loading location. As shown in Fig. 1(d), the side loading was positioned at the end of the top side edge, in fact, a bottom corner of the trapezoid head on the free end. After the loading locations had been determined, the AFM tip was moved laterally to the contact location with a step of 10 nm. Under the programmed control, voltages V_p and V_l, outputs of the piezoresistive force sensor and the photodiode began to be recorded at a frequency of 5 Hz when V_l reached the defined preload value of 0.01 V. During the measurement, the deflection of the AFM cantilever was controlled to keep the voltage output in the linear range of the photodiode.

Data analysis. For the top loading method, the loading force on the AFM tip can be presented as

$$F_t = k_p\delta_p = k_t\delta_t = S_pV_p, \tag{3}$$

where k_t is the total lateral stiffness of the AFM cantilever-tip-contact system and δ_p and δ_t are deflections of the piezoresistive cantilever and AFM cantilever tip, respectively. Here, k_t can be obtained from a sum of stiffness inverses of each part: $k_t=(1/k_{\mathrm{lateral}}+1/k_{\mathrm{tip}}+1/k_{\mathrm{contact}})^{-1}$, where k_{lateral} is the lateral stiffness of the AFM cantilever and its tip lateral stiffness is k_{tip} and k_{contact} is the contact stiffness between the AFM tip and the piezoresistive cantilever surface. k_{contact}, which is proportional to the contact radius[17] and often comparable to k_{lateral} and k_{tip},[18] causes the lateral force calibration to be more challenging because in this case δ_t is not equal to the real lateral deflection associated with the photodiode output. Fortunately, in our method, the lateral conversion factor is directly provided by the ratio of the applied force on the AFM tip and the photodiode's voltage output, regardless of any knowledge of the cantilevers and the laser measuring system. For the top loading method, the force $F_t=S_pV_p$ is applied on the AFM tip, so the conversion factor α can be simply obtained from

$$\alpha = \frac{F_t}{V_l} = S_p\frac{V_p}{V_l}. \tag{4}$$

For the side loading method, in order to reduce the effects of friction force on the contact point, the loading direction is perpendicular to the piezoresistive cantilever. In this case, the lateral force conversion factor α under the side loading is determined from

$$\alpha = \frac{F_s}{V_l} = S_p\frac{V_pL_p\cos\theta}{V_ll_p}, \tag{5}$$

where L_p and l_p are distances from the contact points to the clamping end of the piezoresistive cantilever for top loading and side loading, respectively (shown in Fig. 3).

However, considering that the lateral force is loaded on the side of the tip, not on the tip head of the AFM cantilever, a simple linear transformation of the factor α is given by

$$\alpha' = \alpha\left(1 + \frac{\Delta h}{h + t/2 - \Delta h}\right), \tag{6}$$

where Δh=0.5–0.8 μm is the distance from the contact point to the tip head of the AFM cantilever and t is the cantilever thickness. For the cantilevers used in our experiments h=15.5–17.6 μm and t=0.83–2.28 μm, so an error of the factor α generated from Δh is 2.7%–5%, which is just within an acceptable range.

We quantitatively compared our method with the theoretical method based on the beam mechanics. For the convenient comparison of the normal and lateral conversion factors, the photodiode sensitivity is defined as a ratio of the angular deflection of the AFM cantilever and the photodiode voltage for which the lateral inverse sensitivity is $S_l = \theta_l / V_l$, and the normal photodiode inverse sensitivity is $S_n = \theta_n / V_n$. Here, θ_n and θ_l are the normal and lateral angular deflections of the cantilever, respectively; V_n and V_l are the corresponding photodiode voltage outputs.

The normal spring constant k_n connects the flexural deflection x_n due to an applied normal force F_n, which can be determined by[35]

$$F_n = k_n x_n. \tag{7}$$

So, based on the beam mechanics, Eq. (7) can be presented as

$$F_n = \tfrac{2}{3} k_n l S_n V_n, \tag{8}$$

where l is the effective length of the AFM cantilever. Therefore, the normal inverse sensitivity S_n of the photodiode can be determined from

$$S_n = \frac{3}{2l} \frac{dx_n}{dV_n}. \tag{9}$$

For a cantilever with a rectangular cross section, the lateral force is related to the measured photodiode voltage V_l from

$$F_l = \frac{Gwt^3}{3l(h+t/2)} S_l V_l, \tag{10}$$

where G is the cantilever shear modulus and h is the tip height. Based on the laser beam mechanism, the displacement of the laser spot on the photodiode is decided by the reflecting cantilever's angular deflection and the distance between the reflecting point and the spot position on the photodiode. Normally, the distance can be considered as a constant; so, based on the hypothesis that the photodiode is "rotationally symmetric,"[29] the lateral sensitivity is assumed to be equal to the normal sensitivity. Thus, the lateral force conversion factor α_0 can be calculated from

$$\alpha_0 = \frac{Ewt^3}{3l(h+t/2)} S_n. \tag{11}$$

However, the hypothesis of photodiode symmetry is often not exactly the case due to the possible asymmetry of the laser spot shape as well as the diffraction effects from the cantilever, and may induce errors.

The beam mechanics method requires accurate knowledge of the cantilever's elastic modulus and dimensions. As discussed below, in our experiments, the high-resolution optical microscope is used to measure the cantilever's length, width, and the tip height, and the force oscillation method described in Eq. (1) is used to determine the thickness of the cantilever.

RESULTS AND DISCUSSION

As described above, two loading methods were used in our experiments: top loading and side loading. In the first case, we used Eq. (4) to calculate the lateral force conversion factor. For side loading, considering the loading position and the direction of the loading force, therefore, Eq. (5) was used to calculate the lateral force conversion factor. The inverse sensitivity S_n of the photodiode described in Eqs. (7)–(9) was measured for each AFM cantilever by a linear fit on the plot of the photodiode voltage output versus displacement of the cantilevers. Here, we assumed that the photodiode inverse sensitivities S_l and S_n had the same value in our experiments.

The experimental results are summarized in Table I, which lists the dimensions and the mechanics of the AFM cantilevers. The dimensions, including length L, width w, and tip height h, were measured using the optical microscope. The first flexure resonant frequencies f_0 were used to determine the thickness of the cantilevers from Eq. (1). The normal spring constant k_n and lateral spring constant k_l were calculated from Eq. (2). The last three columns list α_0 cal-

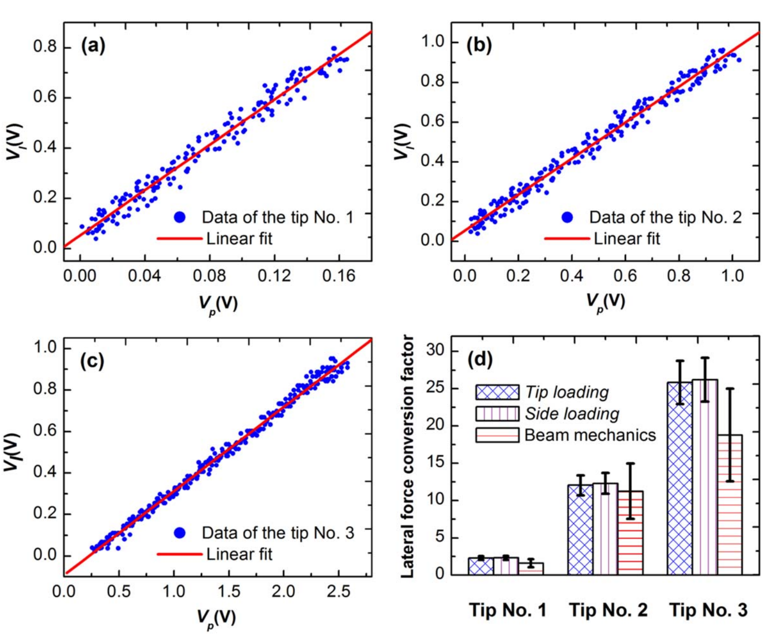

FIG. 4. (Color online) [(a)–(c)] Examples of voltage outputs of the photodiode plotted vs voltage output of the piezoresistive force sensor using cantilever No. 1, No. 2, and No. 3, respectively. The blue solid circles show the data obtained from the experiments using the top loading method. The straight red lines are the linear fit of the corresponding data using the least squares method. (d) The lateral force conversion factors α averaged over ten experimental data repeats for each tip and the lateral force conversion factors α_0 are calculated from Eq. (11) based on the cantilever mechanics.

culated from Eq. (11) based on the beam mechanics, and α measured using the proposed top loading and side loading methods, respectively.

Each cantilever was bent laterally by the piezoresistive cantilever ten times. For each time the lateral force conversion factor was calculated as outlined in Figs. 4(a)–4(c), in which the symbol of the blue solid circles shows data obtained from the experiments using the top loading method. The straight red lines are the linear fit of the corresponding data using the least squares method; their gradients were used to calculate α from Eq. (4). Then, a value of the lateral force conversion factors was averaged from the results of the ten experiment repeats. The lateral force conversion factor α_0 was calculated based on the beam mechanics. Figure 4(d) shows a comparison of the lateral force conversion factors obtained from each method. The top loading and side loading results are approximately the same; the values of the side loading method are just a little higher due to the friction effect not being factored into Eq. (5). But larger differences occur between the measured factors α and α_0 calculated based on the beam mechanics because of cantilever dimension errors and the photodiode's asymmetry sensitivity.

Both methods inevitably have some sources of error. For the proposed method, we need to take into account errors generated by the calibration of the piezoresistive cantilever as well as those from the lateral force calibration of AFM cantilevers, that is, variables S_p, V_p, and V_l for the top loading method, while θ and l need to be added for the side loading method. The errors in these measurements of S_p, V_p, V_l, θ, and l are of the order of 11%, 0.02 V, 0.02 V, 1°, and 2%. Considering the error generated from Δh, the maximum overall error for the calibration of the lateral conversion factor α using the proposed method is 12.4%; it largely depends on the uncertainty of S_p. If an absolute force standard is used to calibrate the piezoresistive force sensor, an error of less than 6% can be expected. Using Eq. (11), the method based on the beam mechanics may yield an overall error as high as 33% with uncertainties: l: 2%, w: 2%, h: 10%, t: 10%, S_n: 10%. For these cantilevers, the two methods actually yield similar results and errors of similar magnitude. However, as the geometry and material composition of the cantilevers become more complicated, the uncertainty of the beam mechanics method will increase significantly. Moreover, this calculation assumes that the photodiode's lateral sensitivity and normal sensitivity are the same, which may not be true. We will test this using a colloidal tip in our future work. In contrast, the piezoresistive force sensor has several attractive features. The most significant fact is that it can provide a force standard for the direct calibration of the lateral force conversion factors without any knowledge of the photodiode or cantilever shape, dimensions, and physical properties, thereby overcoming almost all the difficulties in the calibration of the lateral force measurement.

In summary, we have presented a method to calibrate the lateral force measurement of AFM cantilevers using a piezoresistive force sensor consisting of an off-the-shelf piezoresistive cantilever and its corresponding electronics. This method was used to calibrate three rectangular cantilevers with normal spring constants from 0.092 to 1.24 N/m (lateral stiffness from 10.34 to 101.06 N/m). Compared with the calibration results of the theoretical method based on beam mechanics, the proposed approach provides lateral conversion factor values that are accurate to ±12.4% or better. Moreover, this method can be used to directly calibrate the lateral force regardless of the cantilever's geometry or knowledge of the photodiode detector, thereby enabling an accurate and direct calibration of the lateral force measurement of AFM.

ACKNOWLEDGMENTS

This work was supported by European project NANORAC (Contract No. STRP 013680).

[1] G. Binning, C. F. Quate, and C. Gerber, Phys. Rev. Lett. **56**, 930 (1986).
[2] G. Meyer and N. M. Amer, Appl. Phys. Lett. **57**, 2089 (1990).
[3] T. R. Albrecht, S. Akamine, T. E. Carver, and C. F. Quate, J. Vac. Sci. Technol. A **8**, 3386 (1990).
[4] D. Sarid and V. Elings, J. Vac. Sci. Technol. B **9**, 431 (1991).
[5] J. M. Neumeister and W. A. Ducker, Rev. Sci. Instrum. **65**, 2527 (1994).
[6] J. L. Hazel and V. V. Tsukruk, J. Tribol. **120**, 814 (1998).
[7] J. L. Hazel and V. V. Tsukruk, Thin Solid Films **339**, 249 (1999).
[8] J. P. Cleveland, S. Manne, D. Bocek, and P. K. Hansma, Rev. Sci. Instrum. **64**, 403 (1993).
[9] J. Ruan and B. Bhushan, J. Tribol. **116**, 378 (1994).
[10] J. E. Sader, J. W. M. Chon, and P. Mulvaney, Rev. Sci. Instrum. **70**, 3967 (1999).
[11] P. J. Cumpson, P. Zhdan, and J. Hedley, Ultramicroscopy **100**, 241 (2004).
[12] S. B. Aksu and J. A. Turner, Rev. Sci. Instrum. **78**, 043704 (2007).
[13] D. S. Golovko, T. Haschke, W. Wiechert, and E. Bonaccurso, Rev. Sci. Instrum. **78**, 043705 (2007).
[14] B. Ohler, Rev. Sci. Instrum. **78**, 063701 (2007).
[15] R. S. Gates and M. G. Reitsma, Rev. Sci. Instrum. **78**, 086101 (2007).
[16] E. D. Langlois, G. A. Shaw, J. A. Kramar, J. R. Pratt, and D. C. Hurley, Rev. Sci. Instrum. **78**, 093705 (2007).
[17] R. W. Carpick, D. F. Ogletree, and M. Salmeron, Appl. Phys. Lett. **70**, 1548 (1997).
[18] M. A. Lantz, S. J. O'shea, A. C. F. Hoole, and M. E. Welland, Appl. Phys. Lett. **70**, 970 (1997).
[19] R. G. Cain, S. Biggs, and N. W. Page, J. Colloid Interface Sci. **227**, 55 (2000).
[20] R. J. Cannara, M. Eglin, and R. W. Carpick, Rev. Sci. Instrum. **77**, 053701 (2006).
[21] E. Liu, B. Blanpain, and J. P. Celis, Wear **192**, 141 (1996).
[22] S. Ecke, R. Raiteri, E. Bonaccurso, C. Reiner, H. J. Deiseroth, and H. J. Butt, Rev. Sci. Instrum. **72**, 4164 (2001).
[23] F. Wang and X. Z. Zhao, Rev. Sci. Instrum. **78**, 043701 (2007).
[24] D. F. Ogletree, R. W. Carpick, and M. Salmeron, Rev. Sci. Instrum. **67**, 3298 (1996).
[25] M. Varenberg, I. Etsion, and G. Halperin, Rev. Sci. Instrum. **74**, 3362 (2003).
[26] D. B. Asay and S. H. Kim, Rev. Sci. Instrum. **77**, 043903 (2006).
[27] A. Feiler, P. Attard, and I. Larson, Rev. Sci. Instrum. **71**, 2746 (2000).
[28] N. Morel, M. Ramonda, and P. Tordjeman, Appl. Phys. Lett. **86**, 163103 (2005).
[29] W. H. Liu, K. Bonin, and M. Guthold, Rev. Sci. Instrum. **78**, 063707 (2007).
[30] P. J. Cumpson, J. Hedley, and C. A. Clifford, J. Vac. Sci. Technol. B **23**, 1992 (2005).
[31] S. Jeon, Y. Braiman, and T. Thundat, Appl. Phys. Lett. **84**, 1795 (2004).
[32] Q. Li, K. S. Kim, and A. Rydberg, Rev. Sci. Instrum. **77**, 065105 (2006).
[33] I. Behrens, L. Doering, and E. Peiner, J. Micromech. Microeng. **13**, S171 (2003).
[34] D. A. Mendels, M. Lowe, A. Cuenat, M. G. Cain, E. Vallejo, D. Ellis, and F. Mendels, J. Micromech. Microeng. **16**, 1720 (2006).
[35] C. P. Green, H. Lioe, J. P. Cleveland, R. Proksch, P. Mulvaney, and J. E. Sader, Rev. Sci. Instrum. **75**, 1988 (2004).